ACS APPLIED MATERIALS & INTERFACES

Research Article

www.acsami.org

Facile Synthesis of Enzyme-Inorganic Hybrid Nanoflowers and Its Application as a Colorimetric Platform for Visual Detection of Hydrogen Peroxide and Phenol

Zian Lin,* Yun Xiao, Yuqing Yin, Wenli Hu, Wei Liu, and Huanghao Yang*

Ministry of Education Key Laboratory of Analysis and Detection for Food Safety, Fujian Provincial Key Laboratory of Analysis and Detection Technology for Food Safety, College of Chemistry, Fuzhou University, Fuzhou, Fujian 350116, China

Supporting Information

ABSTRACT: This study reports a facile approach for the synthesis of horseradish peroxidise (HRP)-inorganic hybrid nanoflowers by self-assembly of HRP and copper phosphate ($Cu_3(PO_4)_2 \cdot 3H_2O$) in aqueous solution. Several reaction parameters that affect the formation of the hybrid nanoflowers were investigated and a hierarchical flowerlike spherical structure with hundreds of nanopetals was obtained under the optimum synthetic conditions. The enzymatic activity of HRP embedded in hybrid naonflowers was evaluated based on the principle of HRP catalyzing the oxidation of *o*-phenylenediamine (OPD) in the presence of hydrogen peroxide (H_2O_2). The results showed that 506% enhancement of enzymatic activity in the hybrid nanoflowers could be achieved compared with the free HRP in solution. Taking advantages of the structural feature with catalytic property, a nanoflower-based colorimetric platform was newly designed and applied for fast and sensitive visual detection of H_2O_2 and phenol. The limits of detection (LODs) for H_2O_2 and phenol were as low as 0.5 μM and 1.0 μM by the naked-eye visualization, which meet the requirements of detection of both analytes in clinical diagnosis and environmental water. The proposed method has been successfully applied to the analysis of low-level H_2O_2 in spiked human serum and phenol in sewage, respectively. The recoveries for all the determinations were higher than 92.6%. In addition, the hybrid nanoflowers exhibited excellent reusability and reproducibility in cycle analysis. These primary results demonstrate that the hybrid nanoflowers have a great potential for applications in biomedical and environmental chemistry.

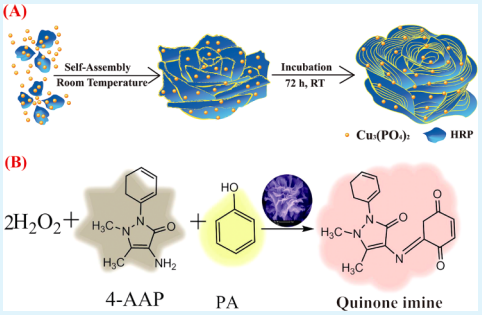

KEYWORDS: *hybrid nanoflower, enzyme, visual detection, H_2O_2, phenol*

INTRODUCTION

The concept of enzyme-embedded nanomaterials, in which enzymes are immobilized in nanostructured materials, has attracted considerable attention because of its potential applications in biocatalysis, proteomic analysis, and sensing.[1−6] Theoretically, enzyme immobilization is expected to have an improvement in enzyme stability and durability, which makes the efficient enzyme reuse economically feasible. Within the past few decades, various novel nanomaterials such as nanoporous silica, nanofibers, magnetic nanoparticles, carbon nanotubes/nanowires, and polymer beads, have been proposed as substrates in the immobilization of enzymes.[7−11] In general, there are several approaches for enzyme immobilization including noncovalent adsorption, covalent conjugation, polymeric entrapment, and cross-linking.[12−15] Although all these approaches exhibited enhanced stability compared to free enzymes in solution, their activities were reduced after immobilization because most of synthetic processes were carried out at harsh conditions (e.g., high temperature and pressure and the use of toxic organic solvents). Less frequently, there are occasions that concern activity retaining of a majority of activity or even activity enhancement after immobilization.[10,16] This apparently hinders wide application of these nanobiocatalytic systems. Therefore, development of a simple and efficient approach for synthesis of enzyme-embedded nanomaterials with enhanced enzymatic activity is highly desirable. Recently, an encouraging breakthrough in synthesis of immobilized enzymes with greatly enhanced activities has been achieved by Zare's group[17] who reported a facile method of preparing enzyme-inorganic hybrid nanostructures with flowerlike shapes, which showed much greater activities than free enzymes and most of the reported immobilized enzymes. Subsequently, Wang et al.[5] also prepared $CaHPO_4$-α-amylase hybrid nanoflowers using the same synthetic route and further enucleated the mechanism for enhanced catalytic activity of immobilized enzyme. Nevertheless, there are few reports[5,6,17] on this approach for the preparation of hybrid nanoflowers and the advantages of enzyme-inorganic hybrid flowerlike nanomaterials have not been fully demonstrated so far. Further

Received: May 5, 2014
Accepted: June 17, 2014
Published: June 17, 2014

development is necessary to explore new applications of this type of hybrid nanoflowers.

Visual detection, in which the presence of target analyte can be directly observed by the naked eye based on color changes, has received increasing interest because of the extreme simplicity and low cost of this type of assay.[18,19] Because both qualitative and semiquantitative assessment can be performed in real time without using any complicated and expensive instruments, visual detection is particularly important in field analysis of point-of-care test and environmental monitoring. More recently, Zare's group[20] reported a method for visual detection of aqueous phenol solutions by using a membrane incorporating laccase nanoflowers, which suggested the feasibility of the enzyme-inorganic hybrid nanoflowers as a colorimetric platform. Despite the attractive features of this technique, additional membrane and a multistep procedure are required, making it less convenient for rapid and on-site detection. Besides, Sun et al.[6] also synthesized multienzyme coembedded organic−inorganic hybrid nanoflowers by using glucose oxidase and horseradish peroxidise (HRP) as the organic components, and copper phosphate ($Cu_3(PO_4)_2 \cdot 3H_2O$) as the inorganic components, which can be further used as a colorimetric sensor for visual detection of glucose. Although two enzymes were used in a one-pot reaction that resulted in less loses of sensitivity of the assay, the morphology and reproducibility of the synthesized nanoflowers were difficult to control because of the usage of multienzyme components. Furthermore, a relatively long analysis time (~25 min) was required in this study.

HRP, as the best-known and most extensively studied groups of enzymes, has received a special attention because of its catalytic ability under a wide range of conditions of temperature, pH, and contaminant concentrations.[21] This versatile enzyme has been widely applied for visual detection of hydrogen peroxide (H_2O_2) and phenols,[22,23] because it can catalyze the oxidation of phenols in the presence of H_2O_2 and chromogenic substrate, yielding a colorimetric change that is detectable by spectrophotometric methods. Conventional colorimetric sensors for detection of H_2O_2[24,25] and phenols are often preformed by free enzyme in bulk solution, but it suffers from several drawbacks such as slow catalytic kinetics, poor stability, and difficult recovery of enzymes.[26] Although these problems can be overcome to some extent by enzyme immobilization, many challenges remain to be faced, which includes the study of new substrates. For analytical purposes, main goals are increase of stability and catalytic activity, elimination of reagent preparation and improvement of reuse.

Inspired by the Zare's studies,[17] herein, a simple approach was developed for the fabrication of enzyme-inorganic hybrid nanoflowers by using HRP as the organic component and $Cu_3(PO_4)_2 \cdot 3H_2O$ as the inorganic component, respectively. The synthesized HRP-embedded hybrid nanoflowers exhibited considerable stability and unusually high catalytic activity. Taking together, a novel strategy of hybrid nanoflower-based colorimetric platform was developed for visual detection of H_2O_2 and phenol. The results suggested that the hybrid nanoflowers displayed both rapid response and sensitivity for the detection of both analytes than the corresponding free enzyme assay.

EXPERIMENTAL SECTION

Reagents and Materials. All other chemicals were of analytical grade or better. Copper sulfate pentahydrate ($CuSO_4 \cdot 5H_2O$), *o*-phenylenediamine (OPD), phenol, and amino acids were purchased from Sinopharm Chemical Reagent, Co., Ltd. (Shanghai, China). HRP (Type E.C. 1.11.1.7, Mw 44 kDa, pI = 7.2, RZ > 3) were obtained from Shanghai Lanji Co. Ltd. (Shanghai, China). Hydrogen peroxide (H_2O_2, 30%, w/v) was purchased from Shantou Xilong Chemical Factory (Guangdong, China) and its concentration was standardized by titration with potassium permanganate. 4-Aminoantipyrine (4-AAP, Mw=203.24, Purity> 98%) was obtained from Shanghai Dibai Chemicals Technology Co., Ltd. (Shanghai, China). The deionized water used in all experiments was purified with a Milli-Q system from Millipore (Milford, MA).

Synthesis. Hybrid nanoflowers were synthesized according to the our previous work with some modifications.[27] Briefly, 30 μL of $CuSO_4$ aqueous solution (120 mM) was added to 4.5 mL of phosphate buffered saline (PBS) (1×, pH 7.4) with different concentration enzyme dissolved. Followed by incubation at 25 °C for 72 h, blue precipitates were collected after centrifugation and dried under vacuum at room temperature.

Enzyme Activity Test. The bioactivity of HRP embedded in nanoflowers was determined by using OPD as the substrate. For this purpose, 100 μg of HRP-inorganic hybrid nanoflowers was transferred to a new vial containing 450 μL of the substrate solution, 100 μM OPD plus 0.12 μM H_2O_2 in PBS (0.1 M, pH 5.8) for different reaction time. Then the reaction was stopped by adding 50 μL of 2 M sulfuric acid and 0.2 M Na_2SO_3. After centrifugation to isolate the nanoflowers, the supernatant was detected by UV/vis absorption and the absorbance was measured at 490 nm. The enzyme units were calculated from the initial rates of OPD oxidation at 490 nm, and the enzymatic reaction was studied by measuring the increase in absorbance of OPD oxidation at 490 nm to obtain the initial reaction rate.[28] As a control, the activity of free HRP in solution was also determined according to the same procedures except for using an equivalent amount of HRP (~16 μg) as a substitute for the nanoflowers.

H_2O_2 and Phenol Detection Test. H_2O_2 detection with HRP-inorganic hybrid nanoflowers was performed as follows: different concentration of H_2O_2 was added into 1.0 mL PBS solution (0.1 M, pH 7.4) containing 100 μg hybrid nanoflowers, 1.0 mM phenol and 4.0 mM AAP, and then incubated at room temperature for 5 min. Then the reaction solution was centrifuged at 10 000 rpm for 10 min, and the absorbance of the supernatant was measured. Similarly, the procedure for phenol detection was same as described above in the presence of 1.0 mM H_2O_2.

Real Sample Preparation and Analysis. For determination of H_2O_2 in normal human serum (donated from Fujian Province Offical Hospital, China), the collected sample was stored at −20 °C and thawed at room temperature before further preparation. As for phenol determination, the sewage was collected from Lianjiang Textile Printing and Dyeing Mill Factory and stored at 4 °C prior to analysis.

The analysis of real samples was performed as follows: To each 1.0 mL serum sample (or sewage) with a 100-flod dilution (diluted with 0.1 M PBS (pH 7.4)), 100 μg hybrid nanoflowers, 1.0 mM phenol (or 1.0 mM H_2O_2) and 4.0 mM AAP was contained. The spiked samples were prepared by the addition of standard H_2O_2 (or phenol) in human serum (or sewage). After incubation at room temperature for 5 min, the reaction solution was centrifuged at 10 000 rpm for 10 min, and the absorbance of the supernatant was measured.

RESULTS AND DISCUSSION

Synthesis and Characterization of HRP-Inorganic Hybrid Nanoflowers. The general scheme for synthesis of HRP-inorganic hybrid nanoflowers was illustrated in Figure 1, in which HRP with different concentrations was added to 4.5 mL of PBS (1X, pH 7.4) containing 30 μL of aqueous $CuSO_4$ (120 mM) solution. After incubation at room temperature for 72h, a large number of blue precipitates were obtained. On the other hand, it is known that HRP can catalyze the oxidation reaction of phenol by H_2O_2 and vice versa. On the basis of the

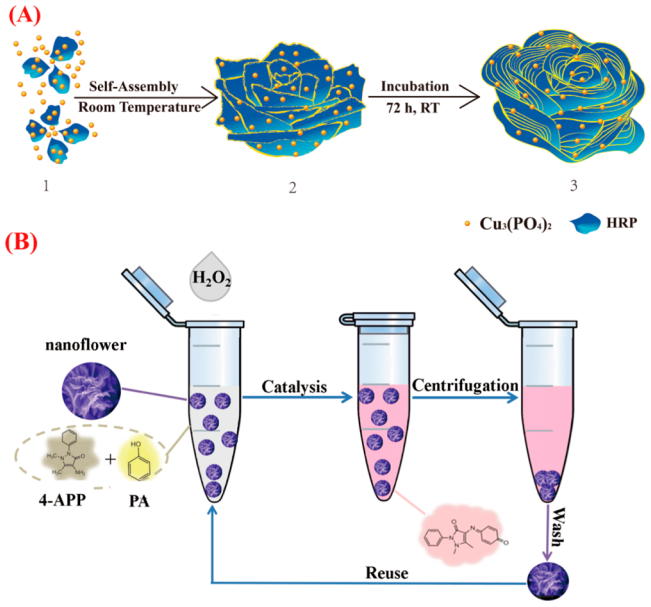

Figure 1. (A) Schematic representation of the synthesis of HRP-inorganic hybrid nanoflowers; (B) a nanoflower-based colorimetric platform for visual detection.

intrinsic peroxidase property of HRP-inorganic hybrid nanoflowers, a reusable colorimetric platform for rapid and sensitive visual detection of the targets was designed as shown in Figure 1B.

To optimize the synthetic condition, the assembly processes which could be mainly influenced by such factors as template concentration and reaction time were examined in detail. HRP concentration ranged from 0 mg/mL to 3.0 mg/mL was first investigated. As shown in Figure S1 (see the Supporting Information), amorphous bulky crystal-like structures, but no nanoflowers, were observed in the absence of HRP (see Figure S1A in the Supporting Information). The flowerlike nanostructures appeared only when HRP was added. However, there was great variation in morphology of the synthesized hybrid nanoflowers by means of regulating the concentrations of HRP. In Figure S1B in the Supporting Information, the separated nanoflowers with an average size of ~20 μm displayed some broken petal-like structures when 0.02 mg/mL HRP was added in the reaction system. With the increase in HRP concentrations from 0.02 to 3.0 mg/mL, the broken petal-like structure gradually forms flowerlike spherical structure (see Figure S1C–E in the Supporting Information). In this case, the obtained hybrid nanoflowers exhibited explicit hierarchical peonylike flower morphologies and the average size of each nanoflower was ~15 μm. The results indicated that HRP concentration added in the reaction synthesis responded to the morphology and size of the hybrid nanoflowers, which would affect the activity and stability of the immobilized enzyme. Meanwhile, reaction time was also studied while keeping HRP concentration (1.0 mg/mL) constant. We expect that a reaction for a longer time until the exhaust of substrate would generate more HRP for nanoflower assembly. To study this, different incubation time (24, 48, and 72 h) was studied, followed by SEM imaging to reveal the structures obtained at each time point. Results shown in Figure S2 (see the Supporting Information) suggest a progressive process of nanoflower assembly. At an early growth stage (24 h, see Figure S2A in the Supporting Information), primary crystals of $Cu_3(PO_4)_2$ were formed. At this stage, only few HRP formed complexes with Cu^{2+} predominantly through coordination of amide groups in the enzyme backbone. These complexes provided a location for nucleation of the primary crystals. With increasing incubation time (48 h, see Figure S2B in the Supporting Information),

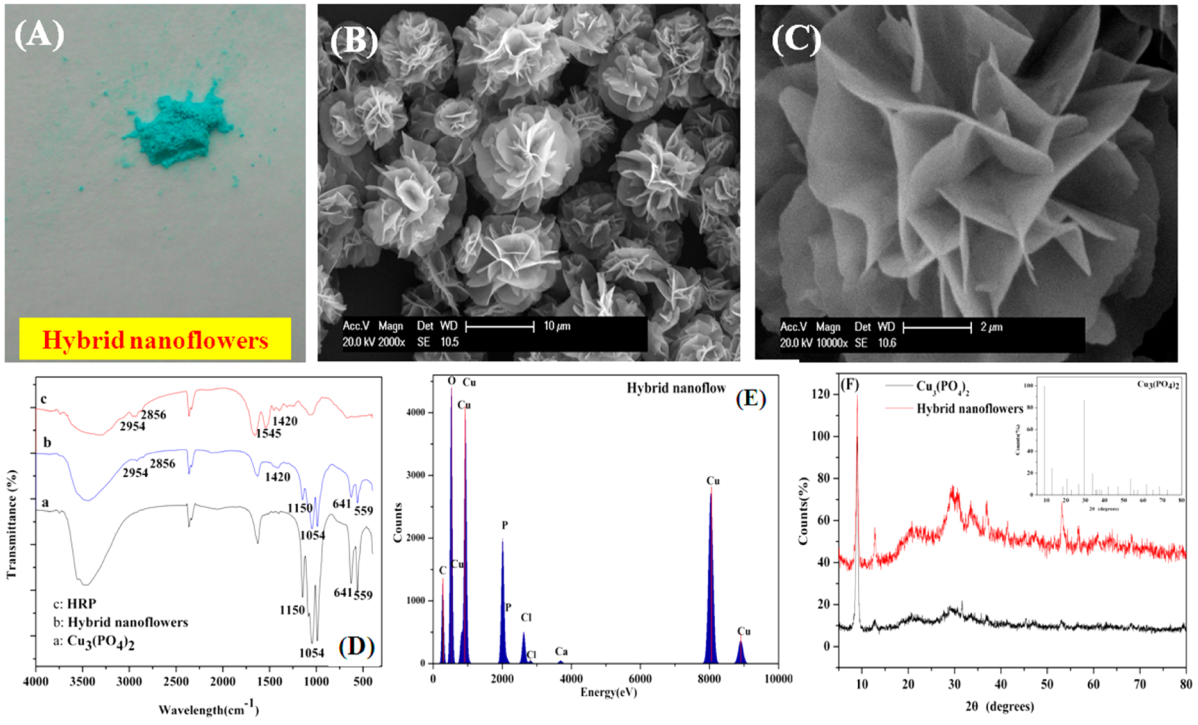

Figure 2. (A) Photograph of the hybrid nanoflowers; (B, C) SEM images of the hybrid nanoflowers; (D) FT-IR spectra of the hybrid nanoflowers; (E) EDX pattern of the hybrid nanoflowers; (F) XRD patterns of the hybrid nanoflowers.

more HRP-Cu^{2+} crystals combined into large agglomerates that formed the primary petals. The kinetically controlled growth of $Cu_3(PO_4)_2$ crystals originated on the surface of these agglomerates, resulting in flowerlike petals to appear in embryo. Anisotropic growth led to complete formation of flowerlike spherical structures when the incubation time reached 72 h (see Figure S2C in the Supporting Information). In this step, HRP induced the nucleation of the $Cu_3(PO_4)_2$ crystals to form the scaffold for the petals, and served as a "glue" to bind the petals together.

Taking the hybrid nanoflowers with 1.0 mg/mL HRP as an example, a full characterization was performed by SEM, FT-IR, EDX, and XRD (Figure 2). Figure 2A showed the photo of the blue HRP-$Cu_3(PO_4)_2$ hybrid nanoflowers, Figure 2B, C displayed the SEM images of the HRP-$Cu_3(PO_4)_2$ hybrid nanoflowers. In the low-resolution SEM images, most of the hybrid nanoflowers were uniform architectures with good monodispersity. However, high-resolution SEM image exhibited hierarchical peonylike flower morphology, which was assembled from hundreds of nanoplates. FT-IR spectroscopy give a direct proof for the formation of the hybrid nanoflowers as shown in Figure 2D, where the strong IR bands (spectrum a) at 1054 and 1150 cm^{-1} were attributed to P−O and P═O vibrations, indicating the existence of phosphate groups. Compared to spectrum a, the typical bands of HRP at 1400−1600 cm^{-1} for −CONH, and 2800−3000 cm^{-1} for $-CH_2$ and $-CH_3$ were observed in spectrum b. Moreover, the hybrid nanoflowers in spectrum b did not show new adsorption peaks and significant peak shift in comparison of spectrum c, indicating HRP was immobilized via self-assembly, instead of covalent bonding. EDX experiment (Figure 2E) revealed that the formed precipitate was constituted by an aggregate with amorphous $Cu_3(PO_4)_2$ crystals that disperse into an organic HRP component. XRD analysis (Figure 2(F) and the inset) confirmed the positions and relative intensities of all diffraction peaks of $Cu_3(PO_4)_2$ matched well with those obtained from the JCPDS card (00−022−0548). The sharp, strong peaks confirmed the hybrid nanoflowers were well crystallized and had high crystallinity after incorporating HRP.

Accordingly, the weight percentage of HRP in the hybrid nanoflowers was further determined by gravimetric methods. The results (see Table S1 in the Supporting Information) showed the weight percentage of HRP embedded in the nanoflowers gradually increased with increasing HRP concentrations, which increased from 0 to 17.2% with HRP concentration changing from 0 to 3.0 mg/mL. However, the corresponding encapsulation efficiency (defined as the ratio of the amount of immobilized enzyme to the total amount of enzyme employed) dramatically decreased from 91.4 to 1.94% (Table S2, in Supporting Information). The results were in accordance with the previous reports,[17,27] and could be explained that the excessive HRP over 1.0 mg/mL was sufficient to exhaust the substrate ($Cu_3(PO_4)_2$). On the basis of the above results, the hybrid nanoflowers with 1.0 mg/mL HRP was chosen as the best for further evaluation and applications considering its good morphology and high weight percentage.

Catalytic Activity and Kinetics of HRP-Inorganic Hybrid Nanoflowers. The catalytic activity of HRP embedded in hybrid nanoflowers was evaluated by using OPD as the substrate, which has been described elsewhere.[28] It is known that in the presence of HRP and H_2O_2, OPD can be oxidized to a water-soluble, yellow-orange product (2,3-diaminophenazine, DAP) that is measured spectrophotometrically at 490 nm, allowing a quantitative analysis of HRP-based systems and monitoring its catalytic kinetics. The absorbance of different systems (the hybrid nanoflowers and free HRP) at DAP peak along time is demonstrated in Figure 3. The plot lies

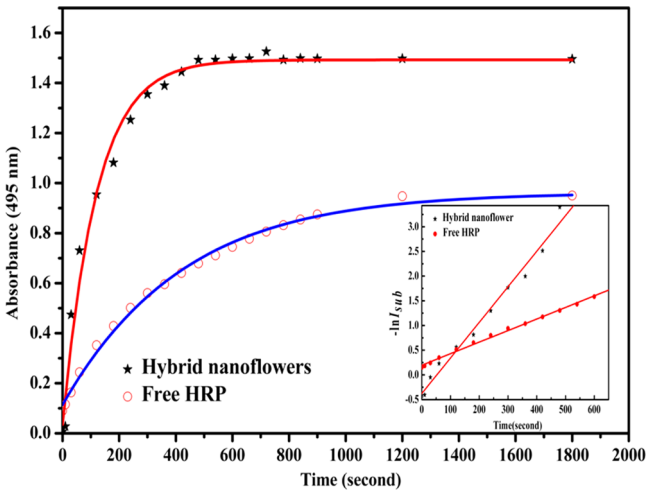

Figure 3. Catalytic kinetics and reaction rate (insert part) of the oxidization of OPD by free HRP and the hybrid nanoflowers; experimental conditions: room temperature, 100 μM OPD, and 0.12 μM H_2O_2 in PBS (0.1 M, pH 5.8) for each system.

on the premise of setting equivalent initial concentrations of OPD to 100 μM. Upon the addition of free HRP, absorbance at 490 nm increased slowly and reached the platform over 900 s. In contrast, in HRP-embedded hybrid nanoflower system, the absorbance platform of DAP could be achieved within 300 s, indicating the high catalytic efficiency of the hybrid nanoflowers. The pseudo-first-order kinetics with respect to OPD could be applied to our experimental system. As shown in the inset figure (Figure 3), the approximately linear shape of the plot of $-\ln I_{sub}$ (I_{sub} is the value obtained by subtracting the real-time absorbance from the saturated one) vs time supports the pseudo-first-order assumption. Based on the linear relationship, the average reaction rate constants (k) were calculated to 7.2×10^{-3} s^{-1} and 2.3×10^{-3} s^{-1} when the hybrid nanoflowers and free HRP were employed, respectively. In addition, the enzymatic activity of HRP in the hybrid nanoflowers was determined to be 15040.5 U/mg, approximately 506% higher than free HRP in solution, where its corresponding activity was 2970.5 U/mg. This enhancement in the catalytic activity of the HRP-embedded hybrid nanoflowers compared to free HRP can be ascribed to the stabilization of nanoflowerlike structure of HRP with high surface area and confinement, resulting in higher accessibility of the substrate to the active sites of HRP.

Visual Detection of H_2O_2 and Phenol. As described above, a colorimetric system involving HRP, co-oxidation of phenol and AAP was developed for the determination of H_2O_2 concentration. On the basis of the same principle, it can also be applied for phenol detection in the presence of H_2O_2. To test the quantitative detection of H_2O_2 using the developed method, different concentrations of H_2O_2 were added to the PBS solution (0.1 M, pH 7.4) containing the HRP-inorganic hybrid nanoflowers and the excessive co-oxidation of phenol and AAP at room temperature. Upon increasing the concentration of H_2O_2, the color of the reaction solution

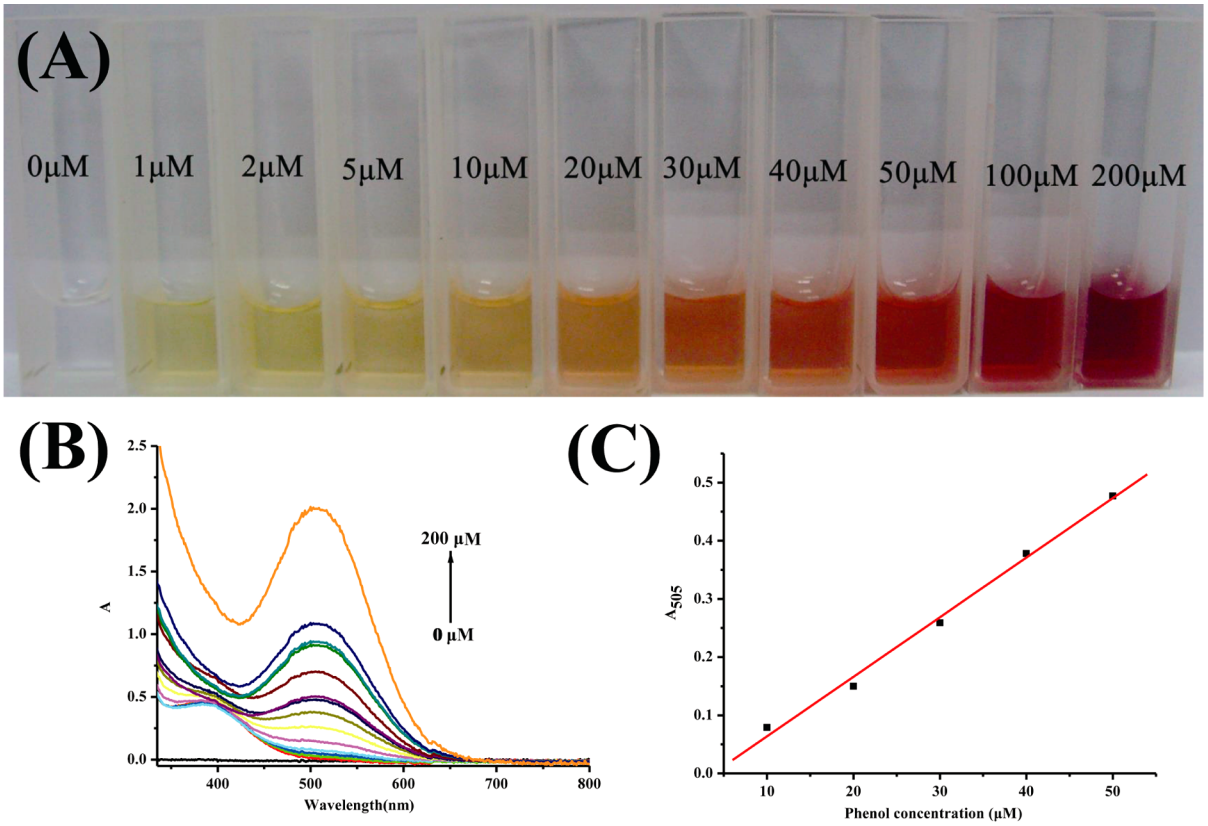

Figure 4. (A) Colorimetric change of the solutions containing hybrid nanoflowers upon the addition of different H_2O_2 concentrations (0−500 μM); (B) UV/vis absorption spectra of the solutions; (C) plot of A_{505} versus H_2O_2 concentration.

gradually changed from colorless to pink (Figure 4A). The high activity of the HRP-inorganic hybrid nanoflowers allowed the fast oxidation reaction, which was completed within 5 min under the employed conditions. There results were further confirmed by UV/vis spectrophotometer. An obvious increase in the adsorption peak at 505 nm was observed by increasing H_2O_2 concentration, which was displayed in Figure 4B. Figure 4C showed the quantitative analysis of H_2O_2 with different concentrations (from 0 to 500 μM in 0.1 M, pH 7.4 PBS). Two linear regressions were found between A_{505} and the H_2O_2 concentration in the range of 0−20 μM (R = 0.9975) and 20−500 μM (R = 0.9997), respectively. H_2O_2 can be detected as low as 0.5 μM by the naked eye, which was much lower than those of previously reported colorimetric H_2O_2 sensors.[29] Significantly, the limit of detection (LOD) obtained in the present work meets well the requirement for early clinical diagnosis (threshold for cell damage: 50 μM).[30] For comparison, determination of H_2O_2 using free HPR solution was also performed by the same procedure. Although a wide linear range of 20−500 μM (R = 0.9950) can be obtained, the LOD of H_2O_2 was ~20 μM (see Figure S3 in the Supporting Information). Furthermore, it took 25 min to complete oxidation reaction. The above results revealed that the nanoflower-based colorimetric sensing platform is highly sensitive. Such high sensitivity and fast oxidation reaction can be related to the high activity of HRP embedded in hybrid nanoflowers. Similarly, the quantitative analysis of phenol was also obtained and the results are shown in Figure 5. An obvious color change switched from colorless to lightyellow, and to pink was observed when the concentration of phenol increased from 0 to 200 μM (Figure 5A), which was also validated by UV/vis spectrophotometer (Figure 5B). A linear relationship was found between A_{505} and the phenol concentration in the range of 0 to 100 μM (R = 0.9998) and its corresponding LOD of 1 μM can be achieved by the naked-eye visualization, which meets the requirement of detection of phenol in environmental water (threshold for phenol: 0.5 mg/L, Chinese National Standards (GB22574−2008)). Compared with the HRP-inorganic hybrid nanoflowers, free HRP solution-based colorimetric system (se Figure S4 in the Supporting Information) showed a narrow linear range (10−50 μM, R = 0. 9960) and a relatively long reaction time (~25 min), even though the same LOD could be obtained by the naked eye. The results can be explained by the fact that the low activity of free HRP in solution brought slow kinetics of the catalytic reactions, thus resulting in slow, gradual changes in color and narrow linear range with low correlation coefficient.

Estimation of the Selectivity and Tolerance Level of Interfering Substances. The selectivity of the proposed method is examined by monitoring the color change of the solution with the presence of H_2O_2 or phenol against other control molecules. As shown in Figure 6A, the presence of the equivalent control molecules (20 μM) caused insignificant color changes of the solutions while the addition of the target H_2O_2 resulted in a clear pink color change of the probe solution. Similarly, as presented in Figure 6B, the color of the solution changed from colorless to light yellow only when phenol was added to the mixture. The addition of other control molecules, in contrast, has no effect on the color of the solutions. The results revealed that the developed approach is highly selective.

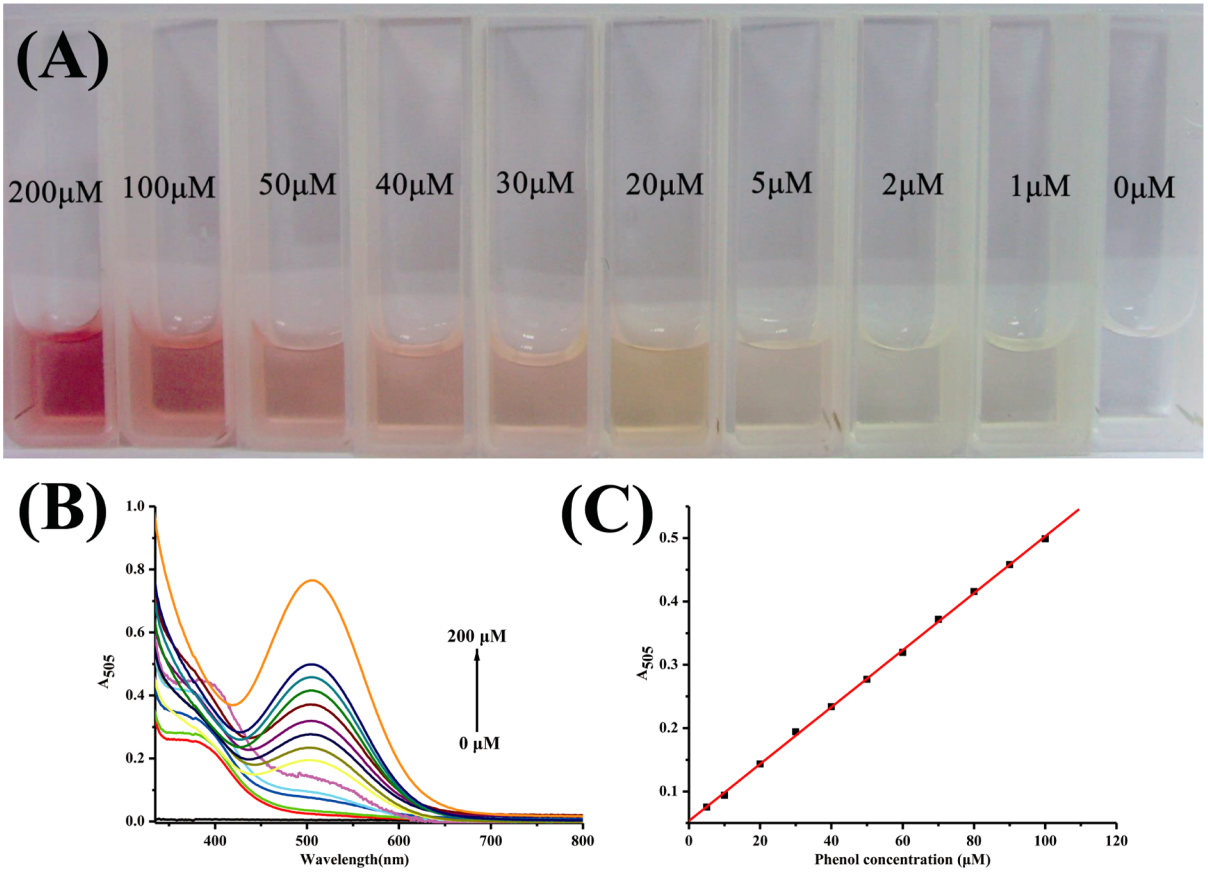

Figure 5. (A) Colorimetric change of the solutions containing hybrid nanoflowers upon the addition of different phenol concentrations (0−200 μM); (B) UV/vis absorption spectra of the solutions; (C) plot of A_{505} versus phenol concentration.

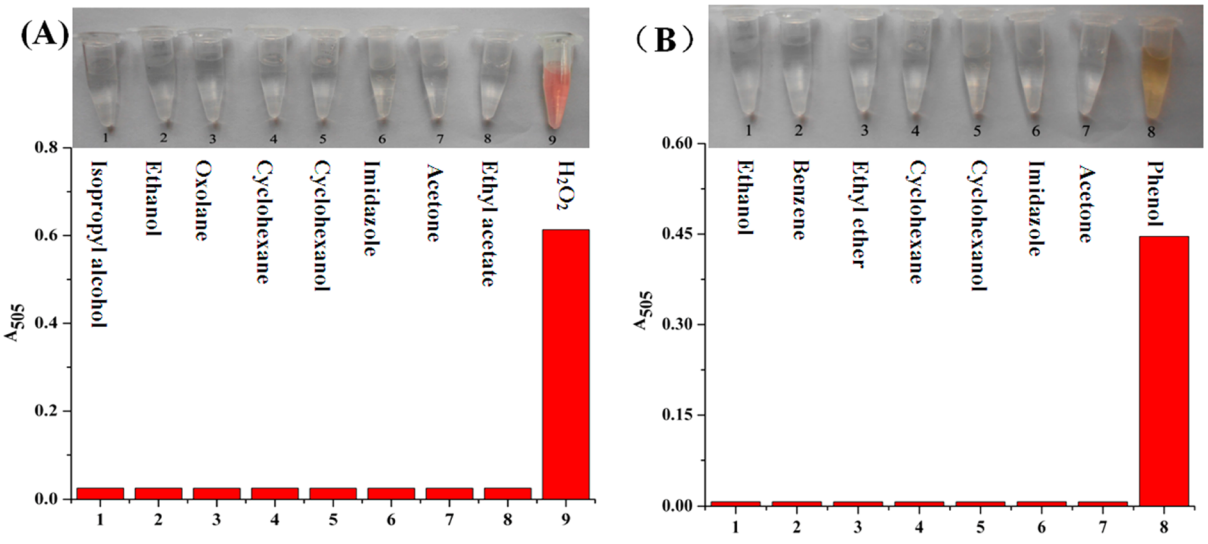

Figure 6. Value of A_{505} and photographs (inset) of the solutions containing (A) H_2O_2, (B) phenol or various species. Concentration of each test substances: 20 μM.

The influence of coexistence substances on the determination of 20 μM H_2O_2 or phenol was investigated with a relative error of ±10.0% (the data were summarized in Tables S3 and S4 in the Supporting Information). As for H_2O_2 visualization, of these tested substances, amino acids (L-Cys, L-Gly, L-Glu, β-Ala, L-Arg, L-Tyr, and L-Try) and sugars (glucose, sucrose, and fructose), which are often existed in human serum, could be allowed to be higher than 200 μM given the tolerance level of ±10%. Some anions/cations (NH_4^+, Cl^-, and NO_3^-) and metal ions except Fe^{2+} and Co^{2+} could be allowed to a 100−500-fold higher concentration in the presence of H_2O_2. Similarly, most of the tested substances except Co^{2+} and Ni^{2+} had not significant effect on the phenol visualization, even though their corresponding concentrations increased from 1 to 10 mM (see Table S4 in the Supporting Information). It should be noted that although the reductive

dx.doi.org/10.1021/am502757e | ACS Appl. Mater. Interfaces 2014, 6, 10775−10782

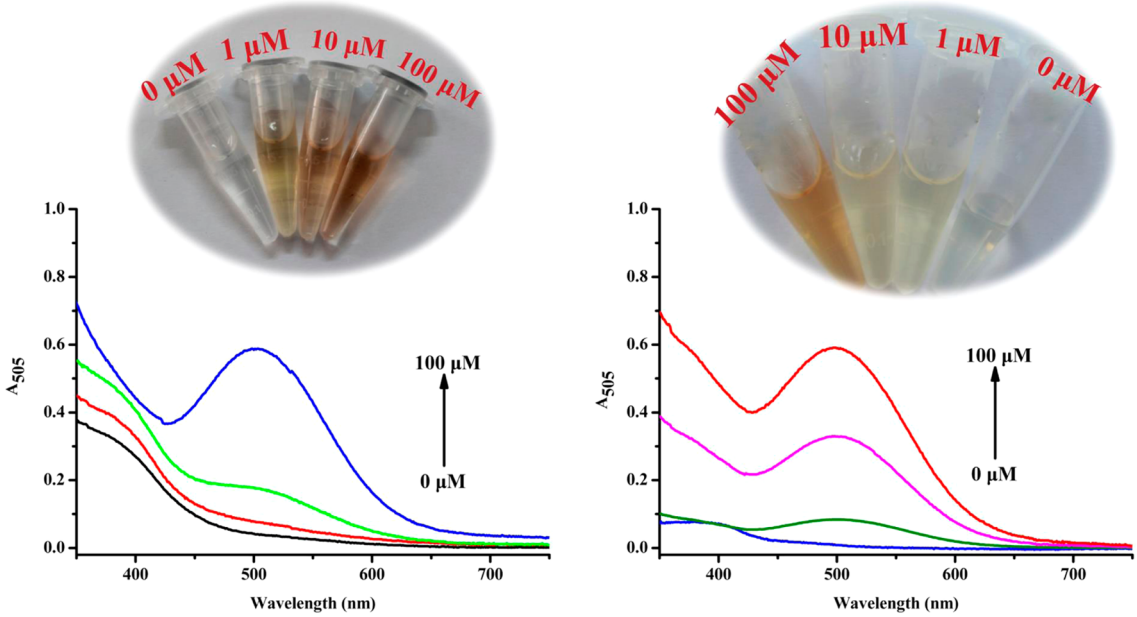

Figure 7. UV/vis absorption spectra of (A) the human serum spiked with different concentrations of H_2O_2 and (B) the sewage spiked with different concentrations of phenol (0, 1, 10, and 100 μM); inset: visual color change of the spiked serum and sewage.

Fe^{2+}, Ni^{2+}, and Co^{2+} has a negative effect on the visual detection of H_2O_2 and phenol, these interferences can be masked by addition of a suitable masking agent (e.g., ethylene diamine tetraacetic acid) prior to target analysis.

Real Sample Analysis. To illustrate the potential application of the hybrid nanoflowers, simple, rapid and cost-effective visualization of H_2O_2 and phenol in real sample was evaluated. It has been reported that H_2O_2 is a byproduct of aerobic respiration and a part of the phageocytic respiratory burst and has been recognized as one of the major risk factors in the progression of disease-related pathophysiological complications such as cancers and cardiovascular disorders.[31] On the other hand, phenol is listed as a high-priority pollutant by the U.S. Environmental Protection Agency and other countries[32] because of its high toxicity. In this experiment, two types of samples, namely, human serum and sewage was tested for each assay. As shown in Figure 7A, no H_2O_2 was detected in the human serum sample and the solution showed colorless. However, the color changes were observed in the spiked serum upon the addition of different concentrations of H_2O_2 (1, 10, and 100 μM). Moreover, the intensity of the pink color depended on the concentration of H_2O_2, which was validated by UV/vis absorption spectra, suggesting the feasibility of the proposed method. Figure 7B showed the visual detection of phenol in sewage. It was clearly observed that no significant color change was detected in sewage. However, upon the addition of different concentration of phenol (1, 10, and 100 μM) in sewage, a gradual color change from light yellow to pink was observed in the spiked sewage. The results supported the view that the HRP-inorganic hybrid nanoflowers can serve as a colorimetric platform for visual sensing of H_2O_2 and phenol. In addition, the recovery of the developed approach was studied and the results showed that the recoveries for H_2O_2 and phenol detection were 95.4−100% (relative standard deviations (RSDs), < 4.8%) and 92.6−102.1% (RSDs < 5.6%), and less than 4.8%, respectively. The results demonstrated that the developed method was reliable, accurate, reproducible, and suitable for the visual detection of the targets in real sample.

Reusability and Reproducibility. To test the reusability of the hybrid nanoflowers and the reproducibility of the detection, a PBS solution with 20 μM H_2O_2 or phenol was used as the sample. Each time after analysis, the hybrid nanoflower was centrifuged and washed with water, exposed to air to dry, and then subjected to the next run. The above-mentioned analysis was conducted once a day for a period of 2 weeks. Figure S5A, B in the Supporting Information showed the absorption intensities of H_2O_2 and phenol at 505 nm within the 10 cycles conducted consecutively in 2 weeks after treatment with the hybrid nanoflowers, and no obvious deformation of morphology was observed (see Figure S6 in the Supporting Information), demonstrating that the nanoflowers process very good mechanical stability. It was observed that the enzymatic activity of HRP embedded in hybrid nanoflowers reduced hardly as the cycle number increased, suggesting the excellent reusability and reproducibility of the hybrid nanoflowers. Apparently, the well preserved analytical ability of colorimetric platform is a result of the high stability of the hybrid nanoflowers at room temperature.

CONCLUSIONS

In summary, we have reported a facile method for the synthesis of HRP-inorganic hybrid nanoflowers by using HRP as the organic components and $Cu_3(PO_4)_2{\cdot}3H_2O$ as the inorganic component. The newly synthesized hybrid nanoflowers presented the hierarchical peonylike flower morphology and exhibited enhanced catalytic activity, compared with that of the free enzyme in solution, which can serve as a colorimetric platform for the visual detection of H_2O_2 and phenol, respectively. The proposed method showed rapid response, excellent selectivity, and sensitivity toward the targets. The successful applications in real sample analysis suggest that the hybrid nanoflowers have great potential as visual sensor platform in biomedical and environmental chemistry.

■ ASSOCIATED CONTENT

Supporting Information

Experimental details, SEM images, and additional spectral data. This material is available free of charge via the Internet at http://pubs.acs.org.

■ AUTHOR INFORMATION

Corresponding Authors

*E-mail: zianlin@fzu.edu.cn.

*E-mail: hhyang@fzu.edu.cn.

Notes

The authors declare no competing financial interest.

■ ACKNOWLEDGMENTS

We gratefully acknowledge the financial support from the National Basic Research Program of China (2010CB732403), the National Natural Science Foundation of China (21375018), the National Natural Science Foundation for Distinguished Young Scholar (21125524), and the Program for Changjiang Scholars and Innovative Research Team in University (IRT1116).

■ REFERENCES

(1) Chiu, C. Y.; Li, Y.; Ruan, L.; Ye, X.; Murray, C. B.; Huang, Y. Platinum Nanocrystals Selectively Shaped Using Facet-Specific PeptideSequences. *Nat. Chem.* **2011**, *3*, 393−399.

(2) Mann, S. Self-Assembly and Transformation of Hybrid Nano-Objects and Nanostructures under Equilibrium and Non-Equilibrium Conditions. *Nat. Mater.* **2009**, *8*, 781−792.

(3) Ge, J.; Lu, D.; Liu, Z.; Liu, Z. Recent Advances in Nanostructured Biocatalysts. *Biochem. Eng. J.* **2009**, *44*, 53−59.

(4) Zeng, J.; Xia, Y. Hybrid Nanomaterials. Not Just a Pretty Flower. *Nat. Nanotechnol.* **2012**, *7*, 415−416.

(5) Wang, L. B.; Wang, Y. C.; He, R.; Zhuang, A.; Wang, X. P.; Zeng, J.; Hou, J. G. A New Nanobiocatalytic System Based on Allosteric Effect with Dramatically Enhanced Enzymatic Performance. *J. Am. Chem. Soc.* **2013**, *135*, 1272−1275.

(6) Sun, J.; Ge, J.; Liu, W.; Lan, M.; Zhang, H.; Wang, P.; Niu, Z. Multi-Enzyme Co-embedded Organic-Inorganic Hybrid Nanoflowers: Synthesis and Application as a Colorimetric Sensor. *Nanoscale* **2014**, *6*, 255−262.

(7) Zhu, J. Y.; Zhang, Y. F.; Lu, D. N.; Zare, R. N.; Ge, J.; Liu, Z. Temperature-Responsive Enzyme-Polymer Nanoconjugates with Enhanced Catalytic Activities in Organic Media. *Chem. Commun.* **2013**, *49*, 6090−6092.

(8) Lee, C. H.; Lin, T. S.; Mou, C. Y. Mesoporous Materials for Encapsulating Enzymes. *Nano Today* **2009**, *4*, 165−179.

(9) Cao, A.; Ye, Z.; Cai, Z.; Dong, E.; Yang, X.; Liu, G.; Deng, X.; Wang, Y.; Yang, S. T.; Wang, H.; Wu, M.; Liu, Y. A Facile Method to Encapsulate Proteins in Silica Nanoparticles: Encapsulated Green Fluorescent Protein as a Robust Fluorescence Probe. *Angew. Chem., Int. Ed.* **2010**, *49*, 3022−3025.

(10) Lei, C.; Shin, Y.; Liu, J.; Ackerman, E. J. Entrapping Enzyme in a Functionalized Nanoporous Support. *J. Am. Chem. Soc.* **2002**, *124*, 11242−11243.

(11) Sun, J.; Ma, Y. T.; Su, Y. J.; Xia, W. S.; Yang, Y. J. Improved Preparation of Immobilized Trypsin on Superparamagnetic Nanoparticles Decorated with Metal Ions. *Colloids Surf., A* **2012**, *414*, 190−197.

(12) Yan, M.; Ge, J.; Liu, Z.; Ouyang, P. Encapsulation of Single Enzyme in Nanogel with Enhanced Biocatalytic Activity and Stability. *J. Am. Chem. Soc.* **2006**, *128*, 11008−11009.

(13) Manesh, K. M.; Santhosh, P.; Uthayakumar, S.; Gopalan, A. I.; Lee, K. P. Electrochemical Biosensing Platforms using Poly-Cyclodextrin and Carbon Nanotube Composite. *Biosens. Bioelectron.* **2010**, *25*, 1579−1586.

(14) Delaittre, G.; Reynhout, I. C.; Cornelissen, J. L. M.; Nolte, R. J. M. Cascade Reactions in an All-Enzyme Nanoreactor. *Chem.—Eur. J.* **2009**, *15*, 12600−12603.

(15) Ma, D.; Li, M.; Patil, A. J.; Mann, S. Fabrication of Protein/Silica Core-Shell Nanoparticles by Microemulsion-Based Molecular Wrapping. *Adv. Mater.* **2004**, *16*, 1838−1841.

(16) Dulay, M. T.; Baca, Q. J.; Zare, R. N. Enhanced Proteolytic Activity of Covalently Bound Enzymes in Photopolymerized Sol Gel. *Anal. Chem.* **2005**, *77*, 4604−4610.

(17) Ge, J.; Lei, J. D.; Zare, R. N. Functional Protein-Organic/Inorganic Hybrid Nanomaterials. *Nat. Nanotechnol.* **2012**, *7*, 428−432.

(18) Song, Y. L.; Zhang, W. T.; An, Y.; Cui, L.; Yu, C. D.; Zhu, Z.; Yang, C. Label-Free Visual Detection of Nucleic Acids in Biological Samples with Single-Base Mismatch Detection Capability. *Chem. Commun.* **2012**, *48*, 576−578.

(19) Yao, Z. Y.; Yang, Y. B.; Chen, X. L.; Hu, X. P.; Zhang, L.; Liu, L.; Zhao, Y. L.; Wu, H. C. Visual Detection of Copper (II) Ions Based on an Anionic Polythiophene Derivative Using Click Chemistry. *Anal. Chem.* **2013**, *85*, 5650−5653.

(20) Zhu, L.; Gong, L.; Zhang, Y.; Wang, R.; Ge, J.; Liu, Z.; Zare, R. N. Rapid Detection of Phenol Using a Membrane Containing Laccase Nanoflowers. *Chem.- Asian J.* **2013**, *8*, 2358−2360.

(21) Ghioureliotis, M.; Nicell, J. A. Assessment of Soluble Products of Peroxidase-Catalyzed Polymerization of Aqueous Phenol. *Enzyme Microb. Technol.* **1999**, *25*, 185−193.

(22) Wang, Q.; Kromka, A.; Babchenko, Q.; Rezek, B.; Li, M.; Boukherroub, R.; Szunerits, S. Nanomolar Hydrogen Peroxide Detection Using Horseradish Peroxidase Covalently Linked to Undoped Nanocrystalline Diamond Surfaces. *Langmuir* **2012**, *28*, 587−592.

(23) Çevik, E.; Şenel, M.; Baykal, A.; Abasıyanık, M. F. A Novel Amperometric Phenol Biosensor Based on Immobilized HRP on Poly(glycidylmethacrylate)-Grafted Iron Oxide Nanoparticles for the Determination of Phenol Derivatives. *Sens. Actuators B* **2012**, *173*, 396−405.

(24) Zhou, L. Z.; Kuai, L.; Li, W. Z.; Geng, B. Y. Ion-Exchange Route to Au-Cu_xOS Yolk-Shell Nanostructures with Porous Shells and Their Ultrasensitive H_2O_2 Detection. *ACS Appl. Mater. Interfaces* **2012**, *4*, 6463−6467.

(25) Li, W. Z.; Kuai, L.; Q, Q.; Geng, B. Y. Ag-Au Bimetallic Nanostructures: Co-reduction Synthesis and Their Component-Dependent Performance for Enzyme-free H_2O_2 Sensing. *J. Mater. Chem. A* **2013**, *1*, 7111−7117.

(26) Klibanov, A. M.; Tu, T.; Scott, K. P. Peroxidase-Catalyzed Removal of Phenols from Coal-Conversion Waste Waters. *Science* **1983**, *221*, 259−261.

(27) Lin, Z. A.; Xiao, Y.; Wang, L.; Yin, Y. Q.; Zheng, J. N.; Yang, H. H.; Chen, G. N. Facile Synthesis of Enzyme-Inorganic Hybrid Nanoflowers and their Application as an Immobilized Trypsin Reactor for Highly Efficient Protein Digestion. *RSC Adv.* **2014**, *4*, 13888−13891.

(28) Romano, M.; Baralle, F. E.; Patriarca, P. Impact of the $R_{286}H$ Substitution on the Biosynthesis and Activity of the Enzyme. *Eur. J. Biochem.* **2000**, *267*, 3704−3711.

(29) Lu, S. G.; Jia, C.; Duan, X. J.; Zhang, X. W.; Luo, F.; Han, Y. W.; Huang, H. Polydiacetylene Vesicles for Hydrogen Peroxide Detection. *Colloids Surf., A* **2014**, *443*, 488−491.

(30) Ijichi, T.; Itoh, T.; Sakai, R.; Nakaji, K.; Miyauchi, T.; Takahashi, R.; Kadosaka, S.; Hirata, M.; Yoneda, S.; Kajita, Y.; Fujita, Y. Multiple Brain Gas Embolism after Ingestion of Concentrated Hydrogen Peroxide. *Neurology* **1997**, *48*, 277−279.

(31) Chang, M. C. Y.; Pralle, A.; Isacoff, E. Y.; Chang, C. J. A Selective, Cell-Permeable Optical Probe for Hydrogen Peroxide in Living Cells. *J. Am. Chem. Soc.* **2004**, *126*, 15392−15393.

(32) Ahmaruzzaman, M.; Gayatri, S. L. Activated Tea Waste as a Potential Low-Cost Adsorbent for the Removal of p-Nitrophenol from Wastewater. *J. Chem. Eng. Data* **2010**, *55*, 4614−4623.